Energy House 2.0

Thermocill

Research Report

by

Dr Majeed Oladokun

and

Dr Richard Fitton

18/11/2020

Contents

1.0 Introduction

The Energy House 2.0 Thermocill Research Report presents the findings of a series of experiments carried out into the thermal and energy performance of Thermocill, an eco-friendly energy saving product that is placed under the window board and above the radiator in a room. The report provides a brief background on how the product works with its benefits, and overview of existing research in the public domain, as well as the core aims and objectives of the research. This is followed by a detailed methodology of experimental design and analytical framework involved in both the measurements and calculation of heat loss, U-values, thermal comfort, and energy savings. The experiments were conducted, over a 10-day period, in the thermal comfort laboratory at the University of Salford Energy House. For the test-series, this study adopts a scenario-based approach using statistical design of experiment with Taguchi orthogonal array design technique. Varying measured variables were selected to include:

- Windows surface temperature, heat flux, and air temperature within the window recess;
- Space thermal comfort parameters: air temperature (0.1m, 1.1m, and 1.7m), globe temperature (1.1m), and relative humidity (1.1m); and
- Heating energy consumption and associated savings.

Further, the result section examines the Thermocill performance from various test scenarios with and without the device in relation to warm-up time, air/surface temperatures, window recess air temperature, heat flux, U-values, thermal comfort, and heating energy consumption. In the concluding part, the report discusses the consequences of the differences between scenarios with and without the Thermocill with respect to the selected performance metrics. Recommendations were finally made on the probable benefits from the use of Thermocill as a low-cost retrofit option for window energy performance improvement.

2.0 Background to the Project

2.1 About the Product

Thermocill is an energy savings product that is designed for installation under the window board and above the radiator in a room. It is made from recycled plastic materials and can be retrofitted to existing homes as well as new builds. In its operation, the product directs the natural convection from the radiator to create a wall of warm air immediately in front of the internal side of the glazed window. It prevents heat loss and cold air entering the room; thus ‘warms up a room faster than normal. With the faster room warms up period, Thermocill possesses the potentials to provide thermal comfort with less energy. Also, Thermocill has a potential to minimise surface condensation from the internal glazed unit, which is often found in newly efficient window systems, however this will not be measured.

Good daylight is essential for improving space lighting performance. Although large windows are preferable for natural lighting, they come with additional heating costs and cold spots near the windows. With the 2025 UK government plan to remove gas appliances from new homes and recent improvements in the standard assessment procedure (SAP 10), Thermocill provides a good opportunity for improving the energy performance of home heating systems.

2.2 Previous Research

Windows undoubtedly provide daylight, solar energy, ventilation and weather protection with satisfactory thermal comfort conditions in residential as well as commercial buildings. Regardless, windows serve as potential “thermal hole” in the building fabrics (Aydın, 2006) causing nearly 20-30% of the total building energy lost through them (Abazari & Mahdavinejad, 2017; Arıcı, Karabay *et al.*, 2015) as well as thermal discomfort (Aydın, 2006). To mitigate these problems, several improvements have been proposed in the form double or multiple glazing, filling cavity with inert gas or surface coatings (Jelle, Hynd *et al.*, 2012). The airflow in naturally ventilated heated buildings is buoyancy driven. Within double glazed window enclosure for instance, the buoyancy-driven airflow between the heated inward and cooled outward panes results in air circulation, leading to alternation of air between the hot and cold sides (Abodahab & Muneer, 1998). This recirculating air current provides additional insulation thereby leading to improved thermal performance of the window assembly. Several research efforts on the air gaps, the gas fill and glass surface treatments have led to improved designs for window energy performance (Jelle, Hynd *et al.*, 2012; Zhang, Bejan *et al.*, 1991).

Also, the convective heat exchange between indoor air and internal building surfaces (e.g., walls, windows, etc.) mainly affects the energy balance in a room (Beausoleil-Morrison, 2002). Accordingly, the surface-to-air exchange determines, for instance, the temperature differentials between room air and building surfaces as well as warm-up period of the room air. Thus, methodology that reduces the cold surfaces (e.g., of windows) will reduce the surface-to-air temperature differentials and warm-up period of the room. Although improved window design increases window energy performance, the design does not eliminate the “thermal hole” defects of glazing on the overall building fabrics energy performance. Other mitigation strategies such as use of window blinds, curtain and installation of radiators near the window have been proposed and tested (Ariosto, Memari *et al.*, 2013; Fang, 2001; Fitton, Marshall *et al.*, 2017; Fitton, Swan *et al.*, 2017; Garber-Slaght & Craven, 2012; Misiopecki, Gustavsen *et al.*, 2013; Wang, Liu *et al.*, 2015). As the window glazing assembly occupies a small part of the external wall thickness, the installation of curtain, blinds, and room radiators near the internal window wall surface leaves “cold spot” in front of the window assembly. For instance, the warm plumes rising from the radiator will be cooled by the cold region in front of the window, causing a reduction in the buoyancy effects near the window. This problem remains a potential issue that leads to large surface-to-air temperature differentials between the window and room air thereby limiting the performance of window assembly.

As Thermocill is installed under the window *cill* and above the radiator in a room, it redirects natural convection from the near-window radiator, creates a wall of warm air immediately in front of the internal side of the glazed window, thereby reducing surface-to-air temperature differentials between the window and room air. Available product information (Fitshow, online), including thermal imaging reports, suggest that Thermocill improves the performance of home heating systems with faster warm-up period and good thermal comfort conditions. However, the evidences were based on the manufacturer’s test results. Thus, the current experiments at Salford Energy House are designed to validate the earlier claims.

2.3 Required Experimental Outcomes

The experiments described in this study demonstrate the following

- Change in warm-up time for each scenario
- Change in U-value for each scenario
- Change in thermal comfort levels for each scenario
- Energy savings potentials of Thermocill between its use and non-usage.

3.0 Experimental Design

3.1 Overview of the Experiment

The experiments took place over a 10-day period in the Salford Energy House thermal comfort laboratory. This area allows the creation of a constant external/internal environment on either side of the test windows. With such steady and replicable conditions, it is easier to measure with close control and accuracy (and thus lower margins of error) the necessary measurands to assess the performance of Thermocill.

3.2 Facilities Used

The Energy House is typical of a terraced house built in Salford in 1919. Because it has been reconstructed in a fully environmentally controllable chamber it provides a unique testing facility for research. The house represents 21% of UK housing stock and was rebuilt using the traditional methods of the time. The house is classed as a hard to treat property in terms of energy efficiency due to the lack of cavity walls.

Unlike test houses built outdoors, conditions in the Energy House can be replicated time and time again whatever the weather is like outdoors. There is also no need for users to wait until the weather conditions meet their requirements as rain, snow, wind and temperature can be specified to high levels of accuracy.

The Salford Energy House provides a unique testing and development facility in which leading researchers can work collaboratively with industry to develop and test new technology and solutions to improve the energy efficiency of existing projects and processes.

Figure 1 – Front Elevation of the Salford Energy House

The Salford Energy House (Fig. 1) is an end of terrace property. This was achieved by the construction of a one-third width full size property, the conditioning

void, next to the Energy House. The conditioning void enables simulation of heat transfer between neighbouring properties.

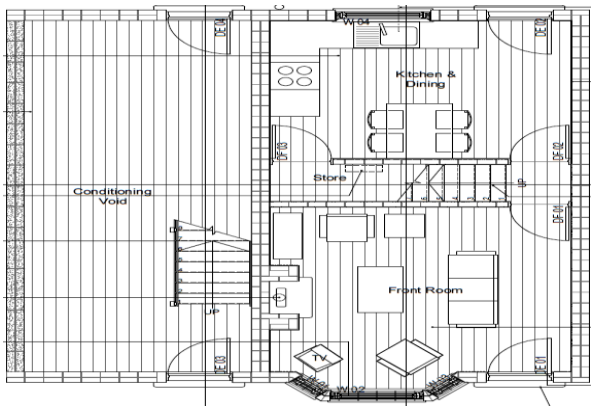

Figure 2 – Ground Floor Plan of the Salford Energy House

On the ground floor (Fig. 2) of the Energy House there is a living room and kitchen diner. Two bedrooms and the bathroom are on the first floor. Details of the original construction, many of which can be changed for tests, are shown below:

Solid Wall Construction

- Bricks: reclaimed handmade clay
- Wall thickness: 230mm
- Bond: English garden wall bond

Roof

- Natural slate
- Sarking felt
- 100mm insulation

Windows

- Glass: single glazed
- Frame: wooden sliding sash

Internal

- Floor: suspended wooden floor
- Walls: wet plaster on brick
- Ceiling: lath and plaster

Electrical Systems

- Traditional 240v ring main
- Voltage optimisation option

Heating Systems

- Gas fired combi condensing boiler band A rated
- Standard wet central heating system
- Standard wall mounted radiators

Climate conditions available in the chamber

- Temperature (-12°C to +30°C) with an accuracy of +/- 0.5°C
- Rain equivalent to 200mm per hour
- Solar
- Light wind

3.3 Experimental Setup and Data Collection Protocol

3.3.1 Performance conceptual framework

Conceptually, Thermocill operates by capturing the buoyant airflow from the radiator and redirecting it towards the window. The redirected airflow forms a vertically upward layer of warm air, which creates a virtual air curtain between the room air and the inner surface of the window. Expectedly, the air temperature in the recess, near the window is reduced. When warm air is kept away from the window, the surface temperature is reduced and invariably minimise the heat flux on the window. Finally, the reduced heat flux on the window will lead to reduction in heating energy utilisation with the use of Thermocill. Thus, the following are the performance assessment objectives of Thermocill:

- Thermocill captures and redirects the buoyant air flow from the radiator, thus there is higher temperature near the Thermocill inlet;
- The use of Thermocill reduces the temperature differences between the room air and the window recess;
- Thermocill use reduces window surface temperature as well as heat flux.

The above objectives guide the selection of measurement points for the thermal performance assessment of Thermocill.

3.3.2 Instrumentation and Test Rig

The experiments follow a similar method to the one used in the previous works by experts at Salford University on windows performance with curtains (Fitton, Swan *et al.*, 2017). The test series were conducted in the thermal comfort laboratory of the Salford Energy House. Fig. 3 shows the experimental setup for the tests. Located on the first floor of the Energy House, the thermal comfort laboratory (Fig. 3a) measures 7661.50 mm by 2791.50 mm (inclusive of the stair hall). The laboratory consists of a two-pane double-glazed window of size 1200mm (width) by 1600mm (height) as shown in Fig. 3a. As the window experiments take place at a micro-environment near the window, the laboratory is partitioned with a fabric curtain (Fig. 3a) across the full height of the room, to keep the heated air within the test area.

Further, the test series involves an array of sensors and datalogging systems. These sensors were set up on standardised rigs (Fig. 3) to match the requirement of ISO9869 for U-value measurement (ISO, 2014), ISO7730 for thermal comfort in buildings (ISO, 2005), and BS EN 17119 for thermographic testing (ISO, 2018). Thus, the following data were collected:

Heat transfer sensors

1. Heat flux measured at the window surface at several points
2. Surface temperature measured on either side of the window
3. Air temperature measured near the Thermocill as well as in the window recess.

Thermal comfort sensors

1. Air velocity sensor
2. Black globe temperature sensor
3. Air temperature sensor
4. Air velocity sensor

5. Relative humidity sensor

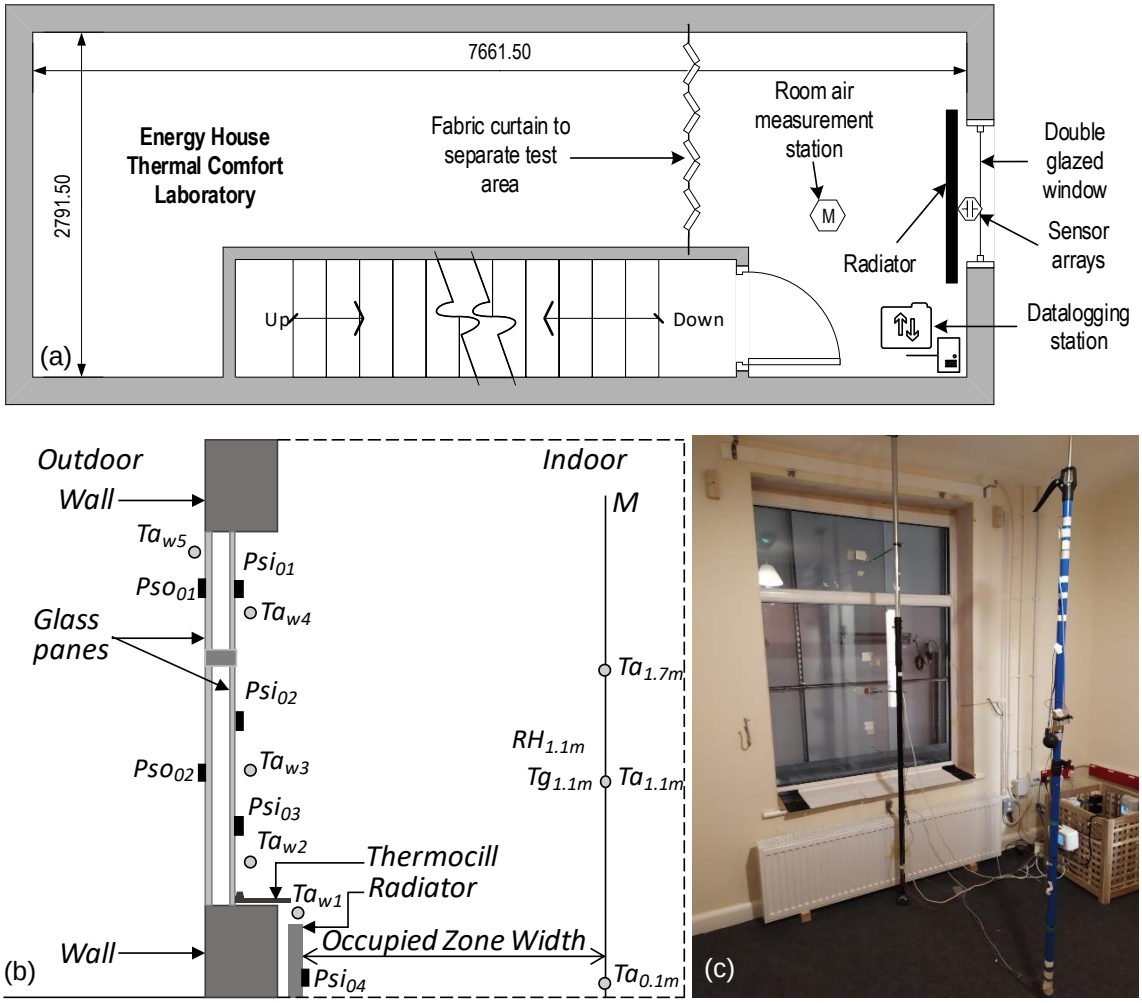

Figure 3. Experimental Setup showing (a) test layout in the Salford Energy House thermal comfort laboratory, (b) simplified schematic of the measurement points, and (c) physical model in the Salford Energy House thermal comfort laboratory.

The surfaces heat transfer was measured with FluxTeq (FluxTeq LLC, online) PHFS-01/ PHFS-01e heat flux sensors. FluxTeq sensors are low-cost, but reliable sensors that combine minimal thickness with excellent sensitivity. They are ideal for long term use in thermal monitoring of windows, walls, ducts, pipes, and other building components. The sensors, which are 32 mm by 30 mm in size also incorporate Type-T thermocouple for measuring the surface temperature. The measurement ranges are +/- 150kW/m^2 for the heat flux and -50 °C to 120 °C for the surface temperature. The sensors are well calibrated by the manufacturer with an accuracy of within 5%; thus, the heat flux measurements were adjusted with the calibration curve details.

FluxTeq heat flux sensors were attached to selected surfaces (marked as Psi_{01}, Psi_{02}, Psi_{03}, Pso_{01} and Pso_{02}) of the double-glazed window under investigation (see Fig. 3a). An additional sensor, Psi_{04} was installed on the surface of the radiator panel. As the FluxTeq incorporates Type-T thermocouple, the sensors were used for simultaneous measurement of heat flux and surface

temperatures at the measurement points. The heat flux sensors were mounted to the surfaces with low tack masking tape.

For thermal comfort assessment, a vertical measurement location (shown as M in Fig. (3a) and blue pole in Fig. (3b)) is installed in the occupied zone. The vertical measurement location was selected to avoid probable effects of locations near heating, ventilation and air conditioning (HVAC) system. It is desirable (see ASHRAE 55 (ASHRAE, 2013a) and ASHRAE 62.1 (ASHRAE, 2013b)) for thermal comfort assessment, to locate the measurement points within the occupied zone, which is defined as the region between 0.075 m and 1.8 m above the floor and no less than 0.6 m away from HVAC equipment, and 0.3 m from internal walls. In the experimental setup for this study, the occupied zone width (Fig. 3) is selected as 1.0 m from the radiator panel and greater than 0.6 m from the adjoining internal walls. Also, for comfort assessment, air temperature sensors were located at 0.1m, 1.1m, and 1.7m (respectively denoted as $Ta_{0.1m}$, $Ta_{1.1m}$, and $Ta_{1.7m}$); while humidity and globe temperature sensor (marked as $RH_{1.1m}$, and $Tg_{1.1m}$ respectively) at 1.1m above the floor level.

One of the key features of Thermocill is its capability to redirect the natural convection from the radiator towards the window recess area, thereby creating a virtual air curtain that separate the warm room air from the cold air near the glazed window. Thus, to capture this stratification effects, air temperatures were measured within the window recess. The measurement locations are marked as Taw_1, Taw_2, Taw_3, and Taw_4 in Fig. (3a). Finally, an additional air temperature sensor was located outside the test room (marked as Taw_5 in Fig. (3a)) to measure the external air temperature. The air temperature was measured with calibrated Type-T thermocouples with an accuracy of 0.4 °C as similar to the one reported by (Fitton, Swan *et al.*, 2017).

The heat flux, surface temperature and air temperature data were logged on three distinct Novus (NOVUS Automation Inc., online) FieldLoggers. This device provides a powerful and efficient data logging of different variable types with high resolution and speed. With its 10/100 Mbps Ethernet interface that allows remote access through a browser (HTTP, FTP, SMTP, SNMP and Modbus TCP), the FieldLoggers were easily incorporated into the sophisticated sensing and logging networks of the Salford Energy house. Thus, the FieldLogger records the data from FluxTeq and Type-T thermocouples (Fig. 3).

Lastly, the test room is heated with a 2000 W 4140 RF water-filled radiator that is placed near the window cill (see Fig. 3). The radiator is equipped with radio frequency controller, which provide wireless thermostatic control as well room set-point monitor. The radiator power consumption and energy use are monitored by power plugs connected to the Building Management System (BMS) of the energy house. With the combination of well-planned experiments, reliable sensing and efficient data logging systems, the experimental protocol in this research reduces the associated uncertainties (Baker, 2009; ISO, 2014) in building fabrics performance assessment.

3.3.3 Experimental Design

The results of experiments depend largely on its design, instrumentation and data logging system. To compliment the high-fidelity sensing and logging system in the energy house, this study adopts a scenario-based approach using statistical design of experiment with Taguchi orthogonal array design technique (Fowlkes &

Creveling, 1995; Phadke, 1995). Using this approach, two design parameters were selected as:

(a) The use of Thermocill with two control levels of ON/OFF conditions, and
(b) Room temperature set-point at two levels of 21 °C and 23 °C.

At each of the experimental trials, the external (chamber) temperature is controlled with the energy house BMS at constant value of 5 °C ± 0.5 °C. Thus, with the two number 2-level design factors, an $L_4(2^3)$ orthogonal array (Phadke, 1995) experimental design (Table 1) was selected for the study. With this array, it is possible to experiment with up to three design parameters, with each of them at two levels.

Table 1. Experimental design for the Thermocill performance assessment

ExpNo	Thermocill	Room Temperature (°C)
1	ON	21
2	ON	23
3	OFF	21
4	OFF	23

For each of the experimental trials shown in Table 1, the Thermocill is adjusted accordingly and room temperature set with the radio frequency controller of the radiator. Thereafter, the earlier described parameters were measured and recorded with the logging system. With the intent of assessing the room warm-up performance of Thermocill, the heating system is shut-down to allow the room return to free-running thermal conditions after each of the experimental trials.

3.4 Data Analysis

For the Thermocill performance assessments, selected metrics include warm-up period, temperature difference between the recess air and room air, windows surface temperature, heat flux, U-value, thermal comfort, and heating energy. These metrics were estimated from the measured variables. The data were analysed in accordance with JCGM 2008 (JCGM, 2008) (uncertainty analysis), ISO7730 (ISO, 2005) (thermal comfort), and ISO9869 (ISO, 2014) (thermal transmittance) with the following outputs for each of the test scenarios:

- Warm-up period in the occupied zone of the test room
- Thermal and/or airflow stratification in the window recess
- Temperature profile (room air, window surface, and window recess)
- Temperature difference between the window recess air and room air
- Heat loss through the window
- Thermal comfort PMV (predicted mean vote), PPD (predicted percentage of dissatisfied), vertical temperature difference and local thermal comfort in accordance with ISO7730
- U-value of window incorporating the Thermocill as an addition to ISO9869

3.4.1 Uncertainty Analysis in Measured and Derived Variables

The reliability of experimental results depends on various uncertainties. For thermal transmittance, these uncertainties range from those associated with sensing equipment, installation of sensing equipment, logging system, correlation between the measurands (e.g., temperature and heat flux), and temporal fluctuation in the measurement (ISO, 2014; JCGM, 2008). These uncertainties can be reduced by selection of instrument with higher accuracy, good installation practices, and repeated measurement over extended period. While estimating uncertainty in single measurand is straightforward, that of derived variable (from the primary measurand) cannot be easily determined (Baker, 2009). For thermal transmittance, ISO9869 (ISO, 2014) provide a range of acceptable uncertainty as between 14% and 28%. An improved method is described in Baker (2009) for uncertainty in the thermal transmittance. However, this method provides uncertainty values that depend on the thermal transmittance itself, which may result in a biased estimate of uncertainty.

This study adopt the method of propagation of uncertainty in measurement (JCGM, 2008; Kline & McClintock, 1953). The method is described as follows:

Assuming a derived variable, R is a function of independent measurands $x_1, x_2, \cdots x_n$, with uncertainties $\Delta x_1, \Delta x_2, \cdots \Delta x_n$; that is, $R = f(x_1, x_1, \cdots x_n)$, then the uncertainty in R, i.e., $U_c(R)$ can be expressed as:

$$U_c(R) = \sqrt{\left(\frac{\partial R}{\partial x_1}\,\Delta x_1\right)^2 + \left(\frac{\partial R}{\partial x_2}\,\Delta x_2\right)^2 + \cdots \left(\frac{\partial R}{\partial x_n}\,\Delta x_n\right)^2} \qquad (1)$$

Where $\partial R/\partial x_1\,, \partial R/\partial x_2\,, \cdots \partial R/\partial x_n$ are the partial derivatives of R with respect to each of the independent measurands. The relative uncertainty can then be computed as $U_c(R)/\,R$.

As repeated measurements were taking over a long period, the uncertainty in the measurands are estimated as a combined uncertainty $\Delta_c x$, with:

$$\Delta_c x = \sqrt{\left(\frac{\sigma_{x,i}}{\sqrt{n}}\right)^2 + (\,\Delta x, i)^2} \qquad (2)$$

Where $U(\mu_{x,i}) = \sigma_{x,i}/\sqrt{n}$ is the standard uncertainty of the average measurement, $\sigma_{x,i}$ is experimental standard deviation and n is the number of observations; and $\Delta x, i$ is the uncertainty in the measurand as obtained from equipment manufacture's specification or calibration curve. In this study, while the uncertainty for heat flux sensors is 5%, that of temperature sensors is 0.4 °C. Equations (1) and (2) can be solved numerically to estimate the uncertainty in any derived variable. The method is also applicable for a single measurand with repeated measurements over a period. Thus, in this study, the method is applied to the measured heat flux as well as the computed U-values.

3.4.2 Analysis of Warm-up period

To assess the warm-up period for each of the test scenarios, this study adopted two methods. Firstly, it was ensured that each experiment starts from when the radiator is switched ON. At the end of the measurement period, the radiator is

switched OFF to allow the room operates at free running-conditions. Secondly, using the air temperature data at 1.1m, the first peak and subsequent drop in the data were identified by a curve-fitting process. The time of peak and drop period were respectively identified as the warm-up and start of steady-state measurement period. In the subsequent analysis the data until steady-state time were excluded for heat flux and U-value computation. These data treatments provide the opportunity to easily capture effects of the Thermocill use, or lack thereof, for the experimental scenarios. Also, for the analysis of heating power consumption and energy use, data for the entire test periods were considered.

3.4.3 Analysis of Thermal Performance

As Thermocill draws its performance strength from redirection of warm air towards the windows surface, it creates virtual air curtain that separate the window recess air from the room air. The effectiveness of these capabilities is assessible from the surface temperature and delta temperature that is defined as the difference between the recess air and room air temperatures. Thus, in this study we examined the thermal performance with the two metrics of surface temperature and delta air temperature.

3.4.4 Analysis of Heat Flux and U-value

There are two basic approaches for estimating U-value from heat flux and temperature measurements: simple averaging method and dynamic method (ISO, 2014). As the series of experiments were conducted under steady-state conditions, the simple averaging method of ISO9869 (ISO, 2014) was adopted as previously reported (Fitton, Marshall *et al.*, 2017; Fitton, Swan *et al.*, 2017) to be suitable for similar experiments done in the thermal comfort laboratory. Using the averaging method, the U-value, U is calculated as:

$$U = \frac{\sum_{i=0}^{t} Q_i}{\sum_{i=0}^{t} T_i - \sum_{i=0}^{t} T_e} \quad (3)$$

Where Q_i, T_i, and T_e are the time-series heat flux, internal temperature and external temperature from the start of steady-state period, i till the end of the test period, t.

The uncertainty $U_c(U)$ in the U-value, is computed using Equations (1) and (2) while the uncertainties, $U_c(Q), U_c(T_i)$, and $U_c(T_e)$, in the independent variables, Q, T_i, and T_e were estimated with Equation (1).

3.4.4 Analysis of Thermal Comfort

In the analysis of thermal comfort, this study employs the metrics described in the ISO7730 (ISO, 2005). The metrics include the predicted mean vote (PMV), the predicted percentage of dissatisfied (PPD), vertical temperature difference and local thermal comfort. Table 2 shows the criteria for acceptable comfort conditions for various categories of indoor environments. All the associated calculations were in accordance with the ISO7730 (ISO, 2005) standard.

Table 2: ISO7730 (ISO, 2005) acceptable comfort criteria for various categories of thermal environment

Thermal Environment Categories	Whole Body Thermal State		Local Discomfort			
	Predicted Mean Vote (-)	Predicted Percentage Dissatisfied (%)	Vertical Air Temperature Difference (°C)	Radiant Temperature Asymmetry from Cool Window (°C)	PD Vertical Temperature Difference (%)	PD Cold Window Surface (%)
A	-0.2 < PMV > +0.2	< 6	< 2	< 10	< 3	< 5
B	-0.5 < PMV > +0.5	< 10	< 3	< 10	< 5	< 5
C	-0.7 < PMV > +0.7	< 15	< 4	< 13	< 10	< 10

4.0 Results and Discussions

4.1 Warm-up period

Fig. 4 compares the room temperature profiles under each of the test scenarios. As shown when Thermocill was installed at room temperature of 21 °C, it takes the room about 78 minutes to warm-up. On the other hand, heating the room without the Thermocill installed resulted in higher warm-up time of up to nearly 95 minutes. Also, using Thermocill while the room setpoint is at 23 °C takes up to nearly 207 minutes to warm-up the room. By contrast, when heating the room at 23 °C setpoint without the Thermocill, a faster warm-up period was recorded at about 168 minutes. This result suggests that at higher room setpoint, the buoyancy driven air current bypasses the Thermocill slot as the buoyant jet flow rates may exceed the capture flow rates by Thermocill.

The time to reach steady-state is consistent with the warm-up period for all the test scenarios. The time to steady-state at 21 °C setpoint is approximately 10 minutes faster when Thermocill was in use as compare when not in use. However, at the room at room setpoint of 23 °C, the time to steady-state was delayed by nearly one hour when Thermocill was in use compare to when not in use. These results may suggest that at higher room setpoint, the buoyancy driven air current bypasses the Thermocill slot as the buoyant jet flow rates may exceed its capture flow rates. This observation may provide a new insight into optimising the design of Thermocill profile for better performance at optimum temperature commonly found in domestic as well as commercial buildings.

With the scenarios of Thermocill OFF set as baseline for each of the room temperature setpoints, the study further compares the performance between the cases of not running Thermocill device with that of running it. Fig. 5 shows that at 21 °C the use of Thermocill warms the room up faster by nearly 20% than its non-usage. By contrast, Thermocill use at higher temperature of 23 °C resulted in about 23% higher warm-up period than when it was not in use.

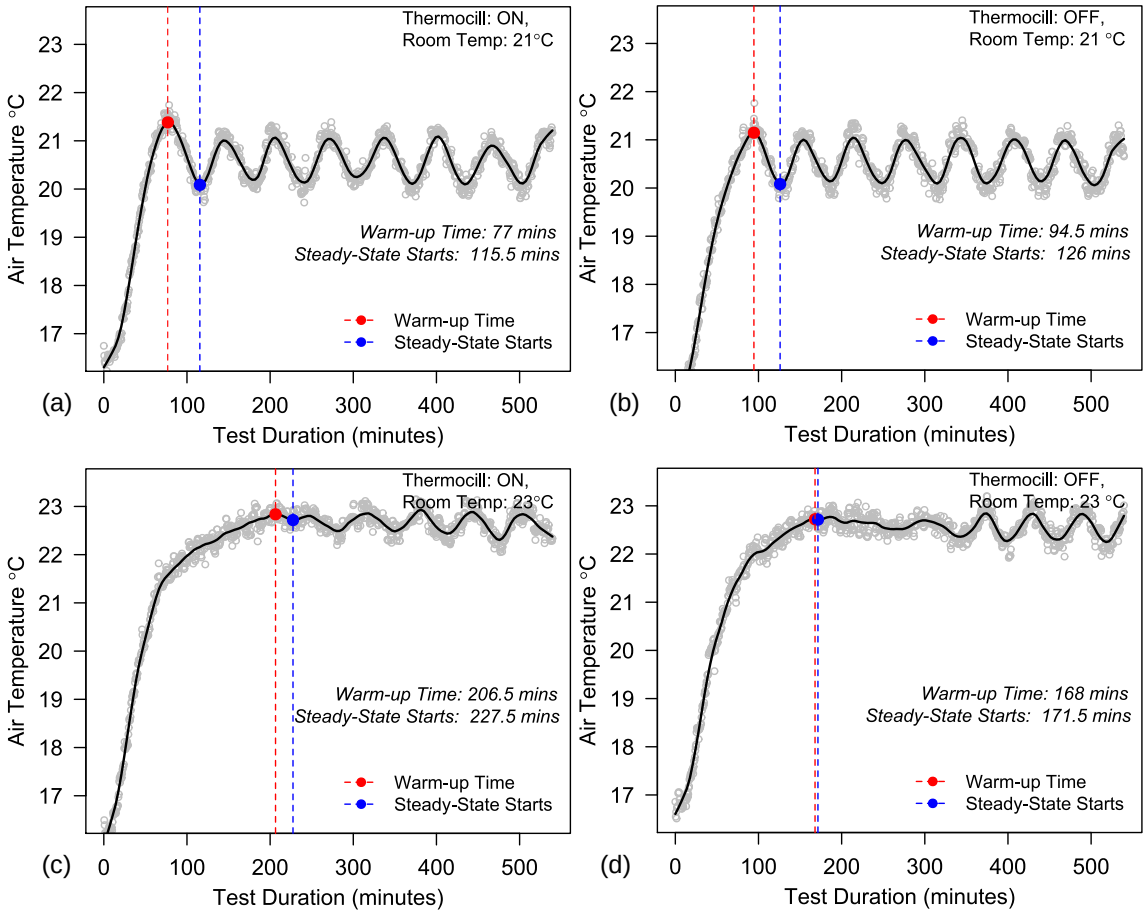

Figure 4. Room air temperature profile showing the time to warm-up the space and attain steady-state temperature when: (a) Thermocill ON, Room temperature at 21 °C; (b) Thermocill OFF, Room temperature at 21 °C, (c) Thermocill ON, Room temperature at 23 °C; and (d) Thermocill OFF, Room temperature at 23 °C

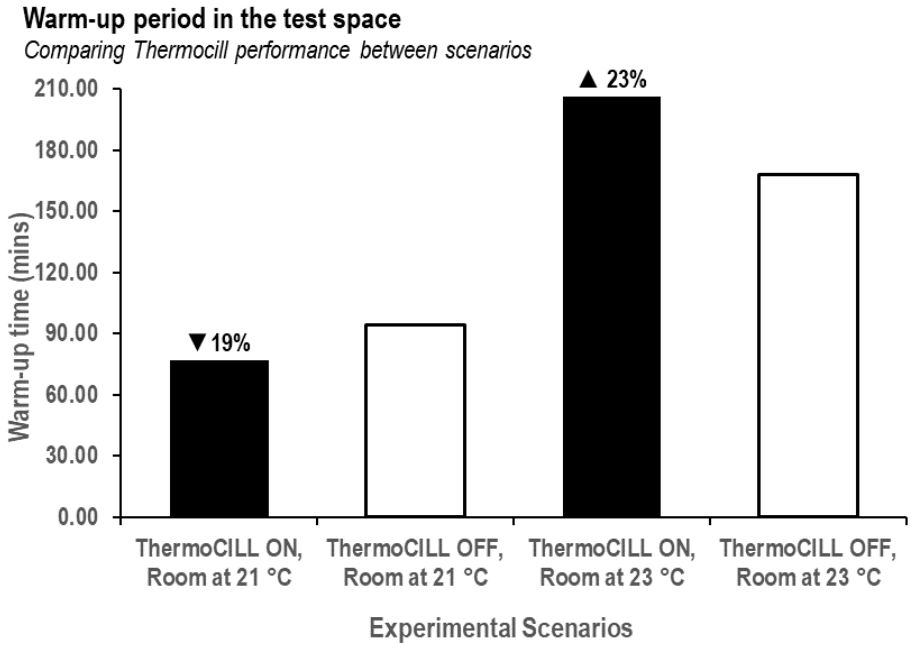

Figure 5. Performance comparison of test scenarios for warm-up time

4.2 Room and Window Recess Air Thermal Stratification

To assess the thermal stratifications under the experimental scenarios, the study presents (Fig. 6) the temporal variation of internal, external and window recess temperatures. As shown, in all the cases, the internal room air temperature and external chamber temperature are steady, thereby confirming the assumption of steady-steady treatment to the experimental data. At the setpoint of 21 °C (Figs. 6a and 6b), the internal air temperature operates at nearly the setpoint of 21 °C. The condition is similar at the setpoint of 23 °C (Figs. 6c and 6d). Also, the results indicate that the window recess air temperatures (marked as bottom-pane (low), bottom-pane (high), and top-pane) exceed that of the room whether the Thermocill is in use or not.

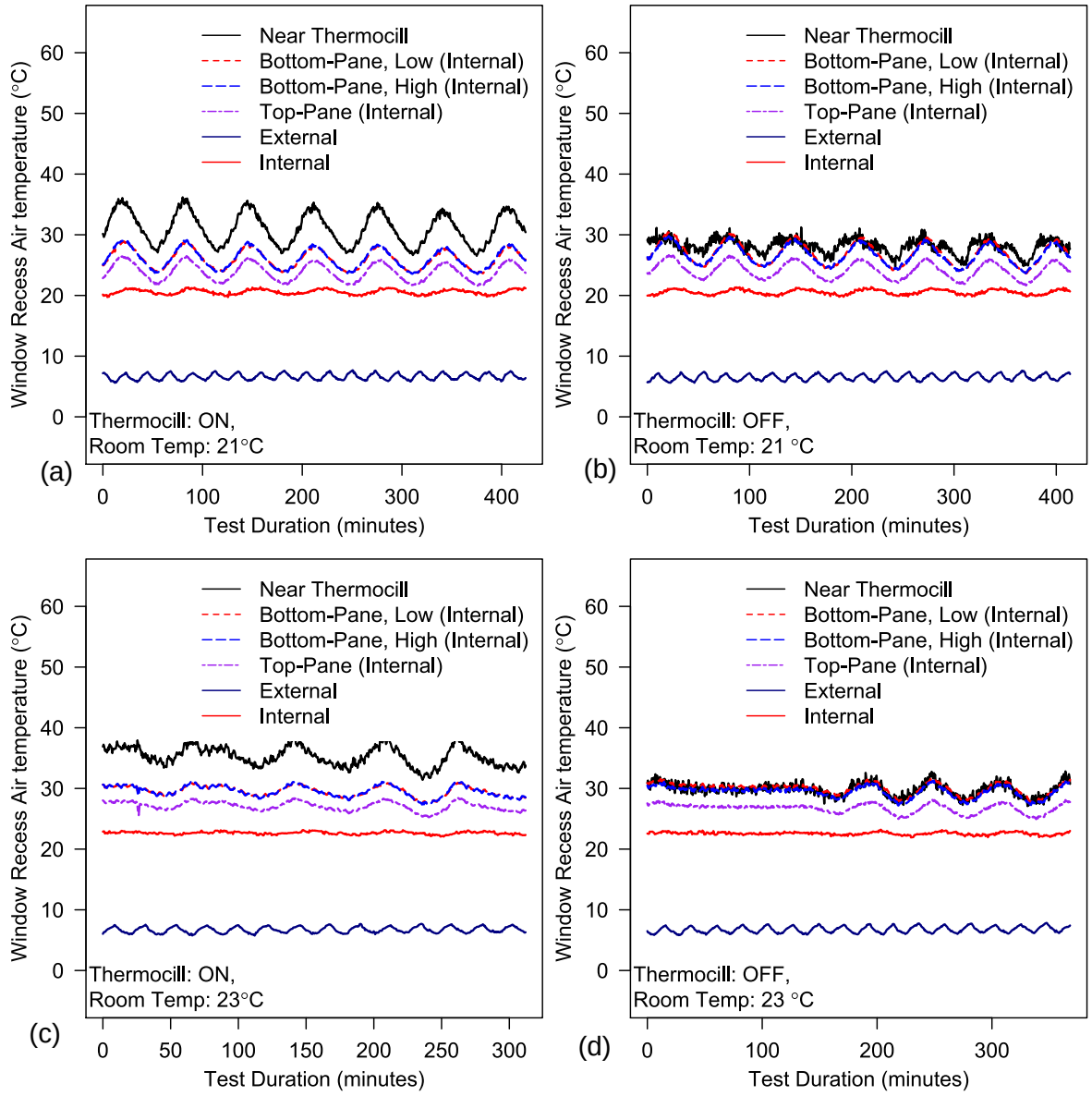

Figure 6. Profile comparing the recess temperature of the double-glazed window, when: (a) Thermocill ON, Room temperature at 21 °C; (b) Thermocill OFF, Room temperature at 21 °C, (c) Thermocill ON, Room temperature at 23 °C; and (d) Thermocill OFF, Room temperature at 23 °C

Further, regardless of the room temperature, the use of Thermocill (Figs. 6a and 6c) did redirects (as shown with temperature near the Thermocill inlet) the warm air towards the window. When the device was in use the air temperature near it peaks at nearly 35 °C. However, when not in use (Figs. 6b and 6d), the air temperature, at the same location near the Thermocill inlet, is equivalent to that of the lower pane of the window, which operate at about 30 °C.

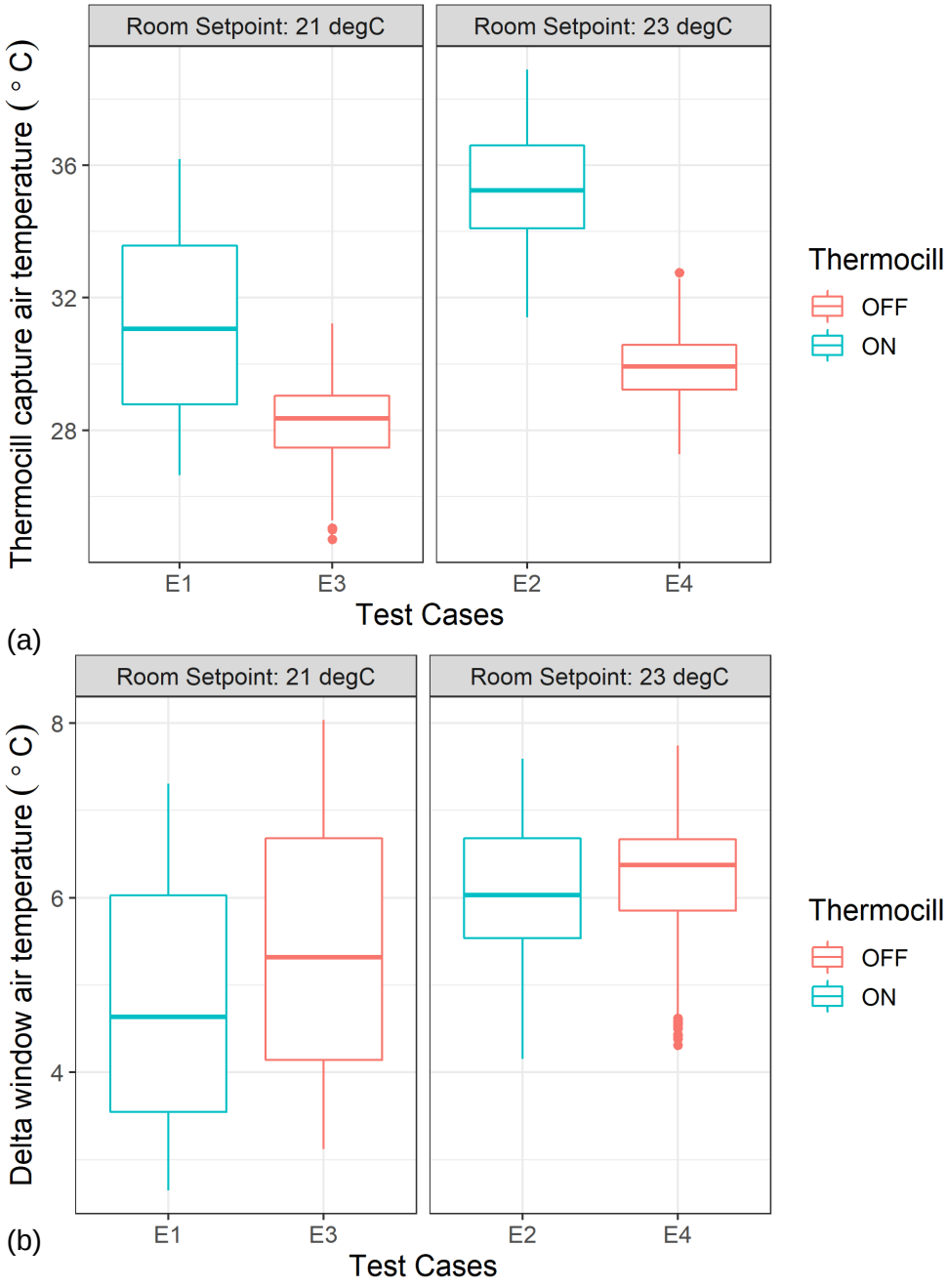

Fig. 7. Comparison between ON/OFF conditions of Thermocill for (a) air temperature (redirected) near Thermocill sensor (maximum is better) and Delta temperature between window recess and room air (minimum is better)

Fig. 8 compares the window surface temperature for the test scenarios. As shown, regardless of the cases, there is evidence of thermal stratification between the lower and upper panes of the window. The surface temperature is highest at the lower pane. The results in Fig. 8 revealed that the bottom pane of the inner glazing is warmer when Thermocill is OFF than when it is ON. As expected, the surface temperature at room setpoint of 23 °C exceeds that of 21 °C. Also, at room setpoint of 21 °C, irrespective of the sensor location on the windowpane, the surface temperature when Thermocill is ON is lower than when it's OFF. At 23 °C, apart from the lower pane, where the surface temperature is lower, there is little difference in the surface temperature between the ON/OFF conditions of Thermocill. These findings further suggest that the redirection of warm air by Thermocill to the window is weaker at higher room setpoint than at lower setpoint.

Overall, the use of Thermocill result in lower window surface temperature than its non-usage. This effect has a potential of reducing the heat loss through the window.

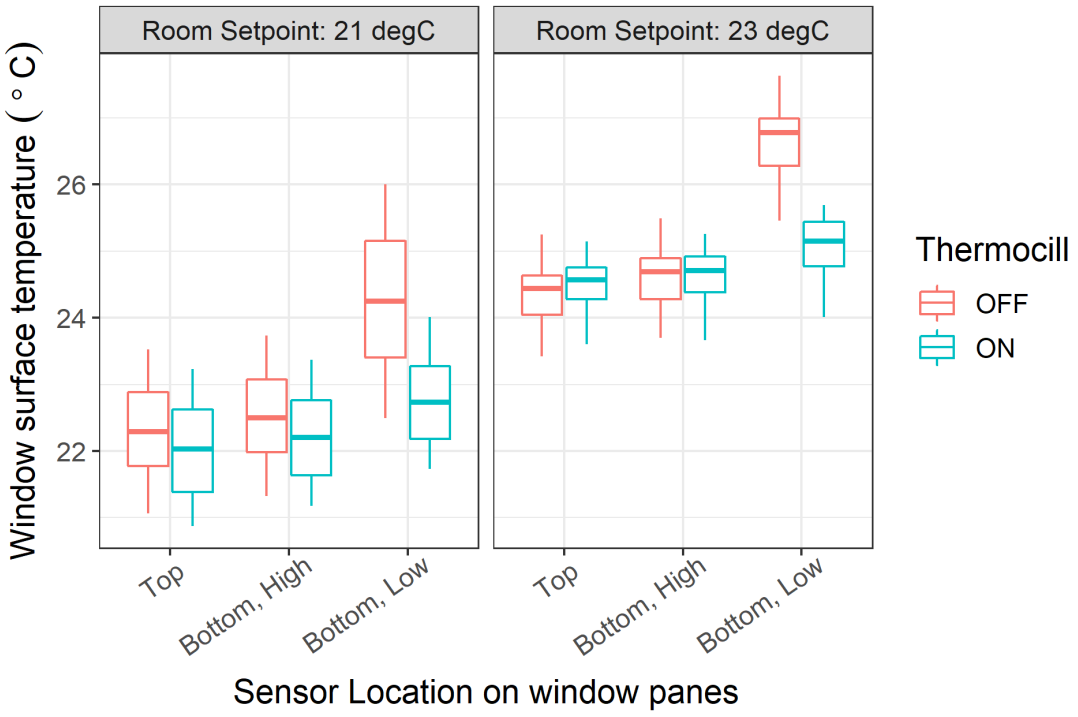

Fig. 8. Comparison between ON/OFF conditions of Thermocill for window internal surface temperature at different sensor locations (minimum is better)

4.3 Thermal Transmission: Heat Flux and U-value

Figs. 9 and 10 present the heat fluxes through the internal and external panes of the window respectively. Also, included in the figures are the 30 minutes moving average of the overall mean heat flux on the panes. The average values were computed from three measurement points on the internal pane and two measurement points on the external panes. The results show that, for the heat flux through the external pane (Figs. 10a and 10b), the 30 minutes moving averages

run around 21 W/m^2 for the cases under room setpoint of 21 °C and at about 25 W/m^2 for the cases under room setpoint of 23 °C (Figs. 10c and 10d). As shown (Figs. 9 and 10), the fluctuation in the heat flux through the internal pane (Fig. 9) is higher than that of the external pane (Fig. 10). Therefore, for improved accuracy of U-value estimate, the study adopts the heat flux through the external pane for the U-value calculation.

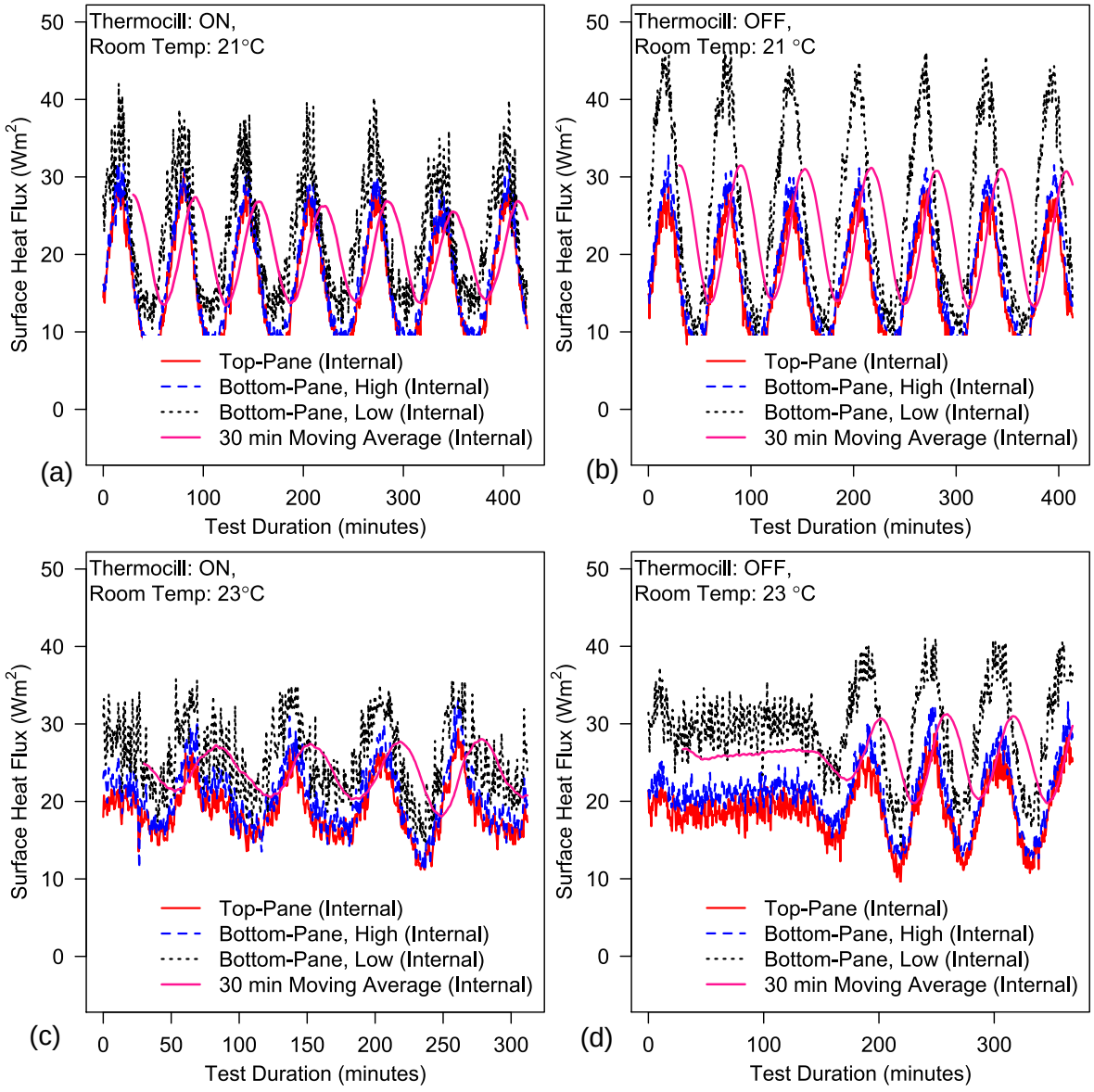

Figure 9. Heat flux profile on the internal pane of the double-glazed window, when: (a) Thermocill ON, Room temperature at 21 °C; (b) Thermocill OFF, Room temperature at 21 °C, (c) Thermocill ON, Room temperature at 23 °C; and (d) Thermocill OFF, Room temperature at 23 °C

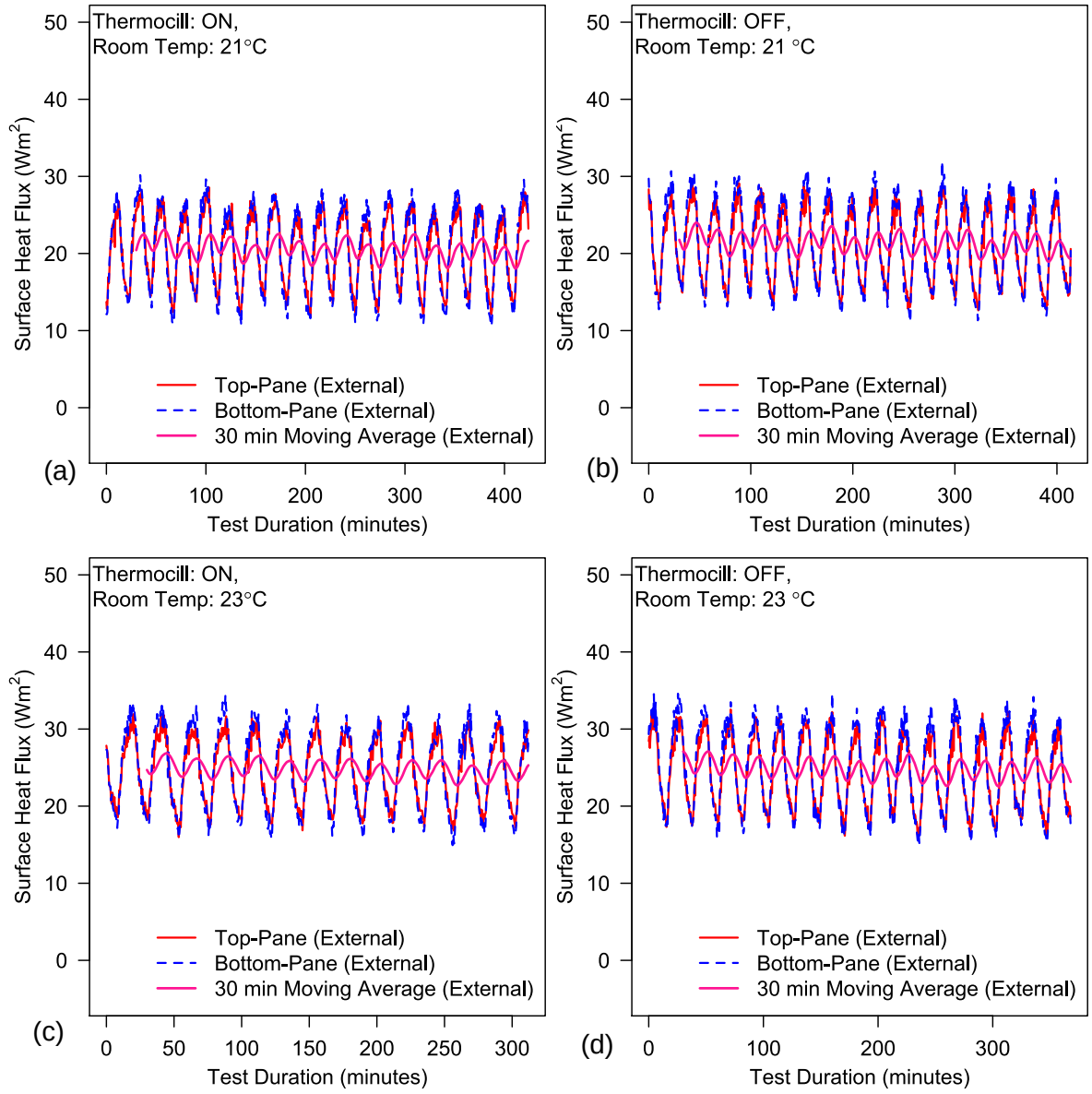

Figure 10. Heat flux profile on the external pane of the double-glazed window, when: (a) Thermocill ON, Room temperature at 21 °C; (b) Thermocill OFF, Room temperature at 21 °C, (c) Thermocill ON, Room temperature at 23 °C; and (d) Thermocill OFF, Room temperature at 23 °C

Fig. 11 compares the thermal performance of the double-glazed window under the tested scenarios. The results shown in Fig. 11 were average values and its uncertainties. For the heat flux measurement, the uncertainty is less than 1% while the uncertainty in the U-value measurement is less than 2%. The results of uncertainty analysis in the U-values are lower than the 14% to 28% recommendation of ISO9869 (ISO, 2014) and 5% presented by Baker (2009). The results thus suggest that the test instruments and experimental protocols are reliable. Further, the uncertainties in the heat fluxes and U-values were lower than the relative difference between the usage and non-usage of Thermocill under the tested temperatures. This result suggests that differences in the U-values are from causes other than the uncertainties in the measurements.

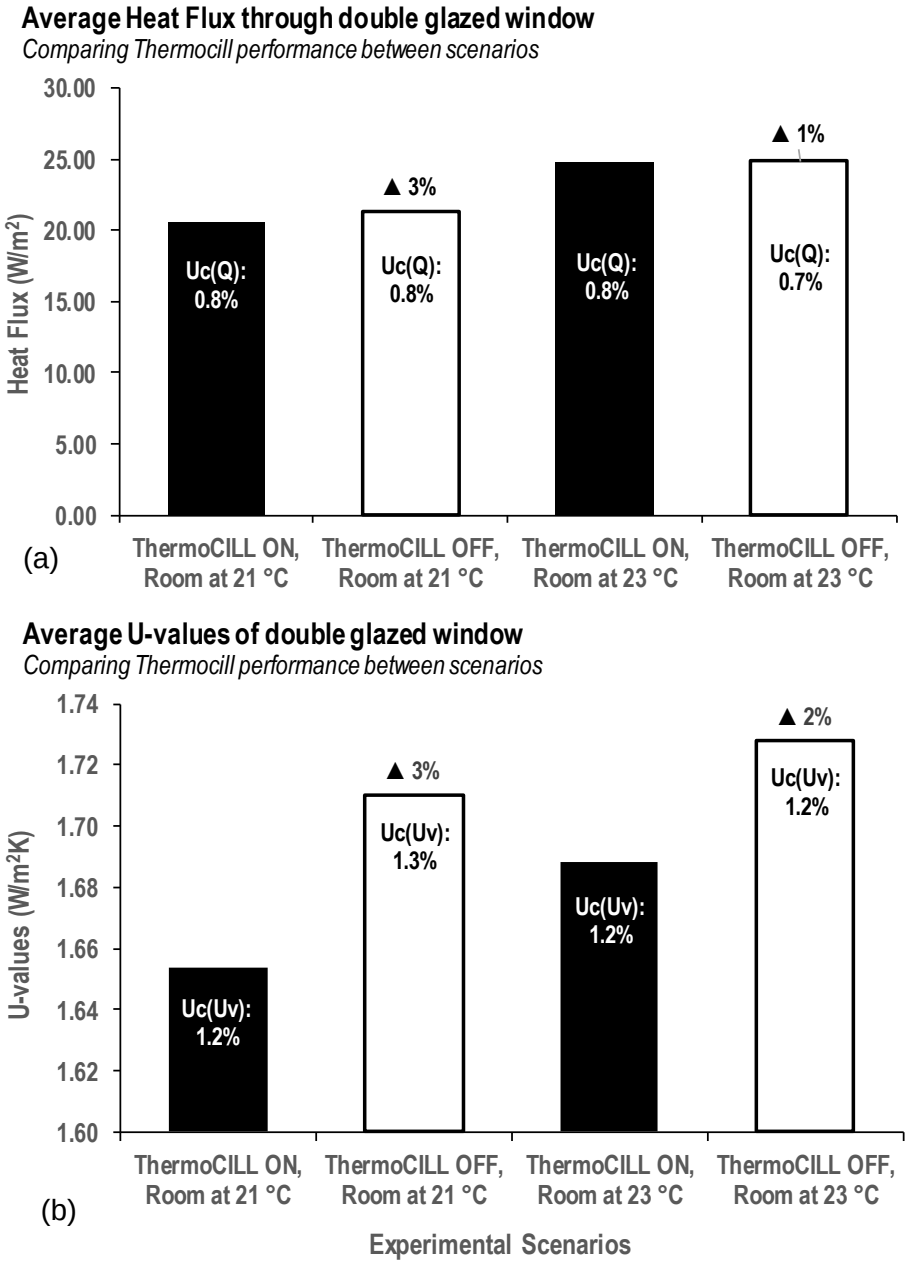

Figure 11. Performance comparison of test scenarios for (a) average heat flux and (b) average U-values

For the heat flux, taking the use of Thermocill as the baseline, the findings show that at 21 °C there is about 3% more heat loss through the window when Thermocill was OFF than when it was ON. For the U-values (Fig. 11b), the results show that at 21 °C the use of Thermocill resulted in a U-value of 1.65 W/m^{2}K for the window, its non-usage leaves the U-value at 1.71 W/m^{2}K. The use of Thermocill thus improved the U-value by about 3%, a value that is consistent with heat transfer through the window. Similarly, at 23 °C, with U-values of 1.69 W/m^{2}K when the Thermocill was ON and 1.73 W/m^{2}K, Thermocill use improves the U-value by about 2%.

4.4 Thermal comfort

Table 3 shows the results of thermal comfort metrics for all the test scenarios. Compare with the ISO7730 (ISO, 2005) acceptable comfort criteria shown in Table 2, the results show that the test room conditions are at least category B (-0.5 < PMV > +0.5) regardless of room temperature setpoint and Thermocill use. The results of PPD follow the same trend with values < 10% in all the test scenarios. The vertical temperature difference, radiant asymmetry from cool window, percent dissatisfied due to vertical temperature difference and cold surface temperature are all within the acceptable range of ISO7730 specification. These results are not surprising as the test room is a controlled environment where all the influencing parameters of thermal comfort are relatively constant.

Although one could compare the thermal comfort metrics between scenarios, such comparison appear unreliable as all the values are well within the comfort performance intervals of the ISO7730 (ISO, 2005). Thus, there is insufficient evidence to support the notion that the use of Thermocill improves thermal comfort conditions.

Table 3: Results of thermal comfort assessments for each of the test scenarios

Test No.	Test Scenarios	Predicted Mean Vote, PMV (-)	Predicted Percentage Dissatisfied, PPD (%)	Vertical Air Temperature Difference (°C)	Radiant Temperature Asymmetry from Cool Window (°C)	PD Vertical Temperature Difference (%)	PD Cold Window Surface (%)
1*	Thermocill ON, Room at 21°C	-0.26	6.40	1.35	-1.68	0.99	0.24
2*	Thermocill ON, Room at 23°C	0.20	5.79	1.79	-2.09	1.44	0.28
3	Thermocill OFF, Room at 21°C	-0.27	6.49	1.34	-2.41	0.98	0.31
4	Thermocill OFF, Room at 23°C	0.18	5.65	1.78	-2.59	1.43	0.33

* Baseline Tests

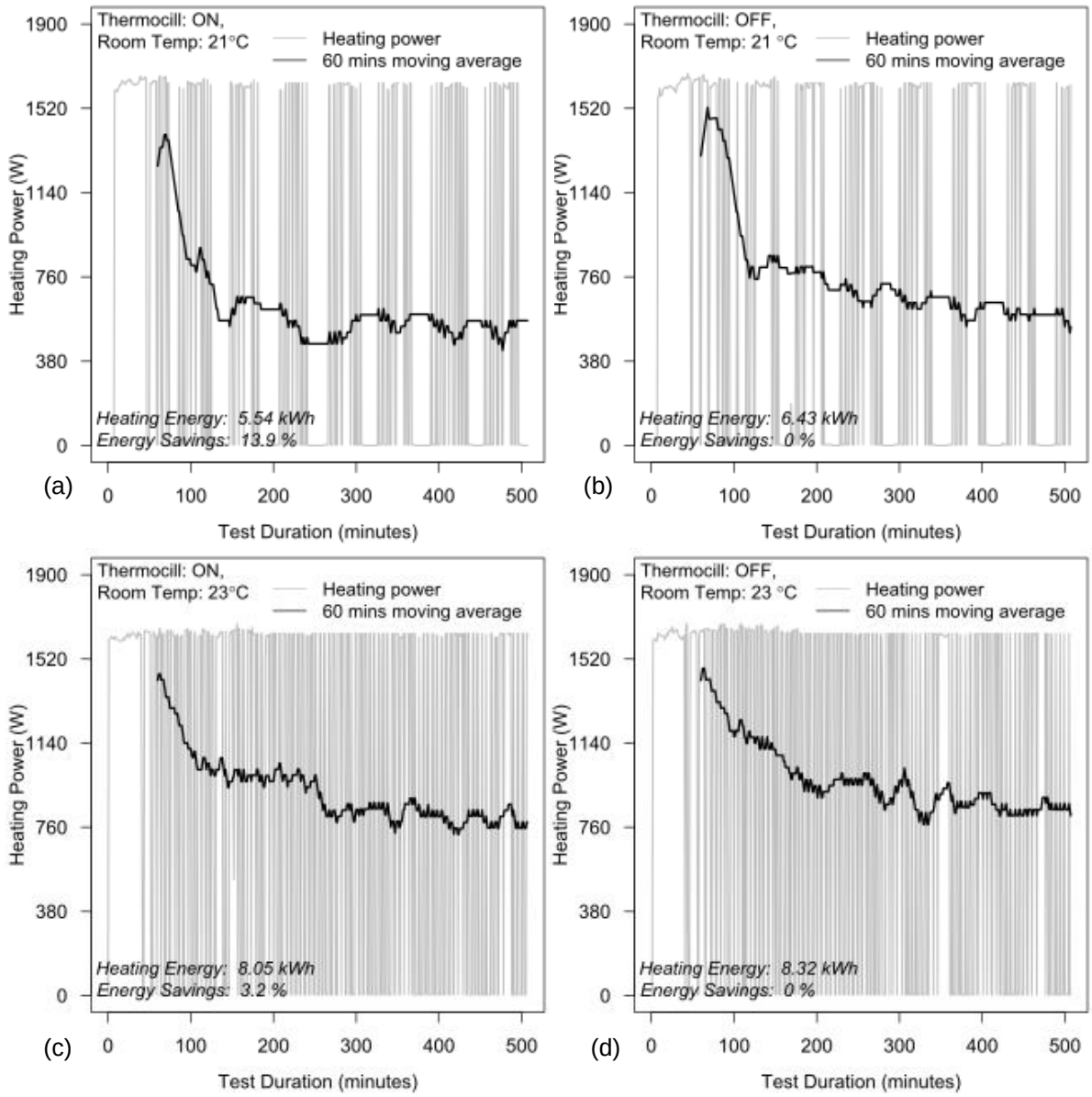

Figure 12. Profile comparing the energy for heating a room with double-glazed window, when: (a) Thermocill ON, Room temperature at 21 °C; (b) Thermocill OFF, Room temperature at 21 °C, (c) Thermocill ON, Room temperature at 23 °C; and (d) Thermocill OFF, Room temperature at 23 °C (Note: the cases with Thermocill OFF, Figs. (b) and (d) were taken as the baseline)

4.5 Heating Power and Energy

Energy efficiency remains one of the goals of building retrofits, it is essential to compare the heating energy consumption of the various test scenarios. Both radiator's power and energy consumption were logged with the BMS in the Energy House. Fig. 12 compares the heating power and energy consumption over the test period. It should be noted that the data covers the entire measurement period as the treatment for steady state condition in heat flux and U-value computation are excluded from the power and energy analysis. In addition to the heating power, Fig. 12 also include the 60 minutes moving average power consumption. The moving average profile is consistent with the warm-up time profile for all the cases.

Comparing between the scenario at 21 °C when Thermocill was ON (Fig. 12a) with that when it was OFF (Fig. 12b), the moving average profile operate at lower level during Thermocill operation than when not in use. For energy savings assessments, the cases with Thermocill OFF (Figs 12b and 12d) were taken as baseline for room setpoints of 21 °C and 23 °C respectively. At the room setpoint of 21 °C, with a total energy of 5.54 kWh when the Thermocill was ON (Fig. 12a) and 6.43 kWh when OFF (Fig. 12b), the use of Thermocill saves about 14% of energy over the 9 hours test period. Similarly, at room setpoint of 23 °C, with a total energy of 8.05 kWh when Thermocill was ON (Fig. 12c) and 8.32 kWh when OFF (Fig. 12d), Thermocill saves about 3% of energy over the 9 hours test period.

The results presented in Fig. 12 agree with findings from warm-up period analysis that at lower room temperature setpoint of 21 °C, Thermocill use performs better than its non-usage; and by contrast the Thermocill performance diminishes at higher room temperature of 23 °C. The poor performance at higher temperature can serve as potentials for optimising the Thermocill design, which may form basis of advanced studies.

5.0 Conclusions

This study forms part of a series of researches on window energy performance improvements by the Salford Energy House team. It assesses the performance of Thermocill at varying test scenarios under controlled conditions of the Salford Energy House's thermal comfort laboratory. The experiments were designed with orthogonal array method and performance assessed under different metrics of warm-up time, thermal stratification, heat flux, thermal transmittance, thermal comfort and energy use. Two types of room temperature setpoints were tested with and without Thermocill use. Surface temperature, heat flux, air temperature and heating energy use were monitored with high precision instrumentation, data logging and experimental protocol. Data were analysed first to identify the warm-up period and start of steady-state condition, which is a pre-requisite to estimating the thermal transmittance by the averaging method of ISO9869.

Findings from the study are summarised as follows:

1. Thermocill indeed diverts warm current towards its inlet as the air temperature near the inlet is higher during the Thermocill use regardless of the room temperature.

2. Use of Thermocill reduces the warm-up period in the test room by nearly 20% at a room temperature setpoint of 21 °C. However, at higher setpoint of 23 °C, the device performs poorly with nearly 23% higher warm-up time. The poor performance at higher temperature may suggest a potential opportunity to optimise the design of the device for improved performance.

3. Evidence of lower temperature difference between the window recess air and room air suggests that Thermocill forms a virtual air curtain that separate window recess from the room air. The virtual separation of window recess from the room air resulted in lower surface temperature, which invariably minimises the heat flux on the window together with its attendant heating energy savings potentials.

4. Comparing usage and non-usage conditions, Thermocill reduces heat loss through double-glazed window by up to 3% and 1% at temperature of 21 °C and 23 °C respectively.

5. The U-value of an unobstructed double-glazed window was reduced by 3% (from 1.71 W/m^{2}K to 1.65 W/m^{2}K) when Thermocill was in use as compared to when not in use at 21 °C and by 2% (from 1.73 W/m^{2}K to 1.69 W/m^{2}K) when the device was in use as compared to when not in use at 23 °C.

6. Under the test conditions, there is insufficient evidence to support the hypothesis that the use of Thermocill improves thermal comfort conditions.

7. Thermocill have a potential to save heating energy depending on the room setpoint temperature. Under the test conditions, the savings could be up to about 14% at 21 °C and 3% at 23 °C.

Further studies are proposed firstly, to investigate on different designs of Thermocill at wider room setpoints and external temperatures as these will assist in design optimisation and the product performance improvements. It would be interesting to examine Thermocill on a lesser performing, such as single glazed, window. The energy savings and U-value savings were very interesting and positive. However, as the reported tests is a short-term in a controlled environment, considering a field trial would be needed to further validate this technology. The interaction with curtains and blinds needs further examination to assess the interaction effects of these combined treatments on window thermal and energy performance.

As the thermal comfort is proved to be non-conclusive, further human centric tests (subjective measurements), in addition to objective measurements may be needed to assess the performance. Modelling and/or simulation can help to incorporate variables other than those tested in the laboratory, as such, further studies on energy and air flow simulation will help not only to improve the thermal performance of Thermocill, it will also assist in assessing wider energy efficiency, carbon savings, lifecycle costing, and payback period from the product.

5. References

Abazari, T., & Mahdavinejad, M. (2017). *Integrated Model for Shading and Airflow Window in BSk*.

Abodahab, N., & Muneer, T. (1998). Free convection analysis of a window cavity and its longitudinal temperature profile. *Energy Conversion and Management, 39*(3-4), 257-267.

Arıcı, M., Karabay, H., & Kan, M. (2015). Flow and heat transfer in double, triple and quadruple pane windows. *Energy and Buildings, 86*, 394-402. doi:https://doi.org/10.1016/j.enbuild.2014.10.043.

Ariosto, T., Memari, A. M., Blansett, K., & Memari, A. (2013). Evaluation of Residential Window Retrofit Solutions for Energy Efficiency. In: Citeseer.

ASHRAE. (2013a). *ANSI/ASHRAE Standard 55-2013: Thermal Environmental Conditions for Human Occupancy*. Atlanta, GA: ASHRAE.

ASHRAE. (2013b). *ASHRAE Standard 62.1-2013 - Ventilation for Acceptable Indoor Air Quality*. Atlanta, GA: ASHRAE.

Aydın, O. (2006). Conjugate heat transfer analysis of double pane windows. *Building and Environment, 41*(2), 109-116. doi:https://doi.org/10.1016/j.buildenv.2005.01.011.

Baker, P. (2009). Research into the thermal performance of traditional windows: timber sash windows. Retrieved from https://ohp.parks.ca.gov/pages/1054/files/6%20hs%20technicalpaper%201.pdf

Beausoleil-Morrison, I. (2002). The adaptive simulation of convective heat transfer at internal building surfaces. *Building and Environment, 37*(8), 791-806. doi:https://doi.org/10.1016/S0360-1323(02)00042-2.

Fang, X. D. (2001). A study of the U-factor of a window with a cloth curtain. *Applied Thermal Engineering, 21*(5), 549-558. doi:Doi 10.1016/S1359-4311(00)00071-5.

Fitshow. (online). Energy-saving Thermocill 'warms up a Room Faster'. Retrieved from https://www.fitshow.co.uk/news/exhibitors/10-exhibitor-news/481-energy-saving-Thermocill-warms-up-a-room-faster

Fitton, R., Marshall, A., Benjaber M., & Swan W. (2017). A study of the thermal performance of tweed curtains under controlled conditions. in *PLEA 2017*. Available at: http://nceub.org.uk/PLEA2017/proceedings/PLEA2017_proceedings_volume_II.pdf.

Fitton, R., Swan, W., Hughes, T., & Benjaber, M. (2017). The thermal performance of window coverings in a whole house test facility with single-glazed sash windows. *Energy Efficiency, 10*(6), 1419-1431.

FluxTeq LLC. (online). PHFS-01e Heat Flux Sensor. Retrieved from https://www.fluxteq.com/phfs-01e-heat-flux-sensor

Fowlkes, W. Y., & Creveling, C. M. (1995). *Engineering Methods for Robust Product Design: Using Taguchi Methods in Technology and Product Development*: Addison-Wesley Publishing Company.

Garber-Slaght, R., & Craven, C. (2012). Evaluating window insulation for cold climates. *Journal of Green Building, 7*(3), 32-48. doi:10.3992/jgb.7.3.32.

ISO. (2005). *ISO 7730: Ergonomics of the thermal environment Analytical determination and interpretation of thermal comfort using calculation of the PMV and PPD indices and local thermal comfort criteria*: International Standard Organisation.

ISO. (2014). *ISO 9869-1:2014 Thermal insulation -- Building elements -- In-situ measurement of thermal resistance and thermal transmittance -- Part 1: Heat flow meter method*: International Standard Organisation.

ISO. (2018). *BS EN 17119:2018 Non-destructive testing. Thermographic testing. Active thermography*: International Standard Organisation.

JCGM. (2008). *JCGM 100: 2008 (GUM 1995 with minor corrections) Evaluation of measurement data-Guide to the expression of uncertainty in measurement*: Joint Committee for Guides in Metrology.

Jelle, B. P., Hynd, A., Gustavsen, A., Arasteh, D., Goudey, H., & Hart, R. (2012). Fenestration of today and tomorrow: A state-of-the-art review and future research opportunities. *Solar Energy Materials and Solar Cells, 96*, 1-28. doi:https://doi.org/10.1016/j.solmat.2011.08.010.

Kline, S. J., & McClintock, F. A. (1953). Describing uncertainty in single sample experiments. *Mech. Engineering, 75*, 3-8.

Misiopecki, C., Gustavsen, A., & Jelle, B. P. (2013). Investigating influence of different shading devices on window thermal performance. in *13th Conference of International Building Performance Simulation Association, Chambéry, France, August 2013*.

NOVUS Automation Inc. (online). FieldLogger - Industrial Multichannel Data Logger. Retrieved from https://www.novusautomation.com/site/default.asp?TroncoID=621808&SecaoID=819191&SubsecaoID=0&Template=../catalogos/layout_produto.asp&ProdutoID=506190&idioma=1

Phadke, M. S. (1995). *Quality Engineering Using Robust Design*: Prentice Hall.

Wang, D., Liu, Y., Wang, Y., Zhang, Q., & Liu, J. (2015). Theoretical and experimental research on the additional thermal resistance of a built-in curtain on a glazed window. *Energy and Buildings, 88*, 68-77. doi:10.1016/j.enbuild.2014.11.047.

Zhang, Z., Bejan, A., & Lage, J. L. (1991). Natural convection in a vertical enclosure with internal permeable screen. *Journal of Heat Transfer, 113*(2), 377-383. doi:10.1115/1.2910572.